REPORT DOCUMENTATION PAGE

Form Approved OMB NO. 0704-0188

1. REPORT DATE (DD-MM-YYYY)	2. REPORT TYPE	3. DATES COVERED (From - To)
	New Reprint	-

4. TITLE AND SUBTITLE

Effects of pelletization pressure on the physical and chemical properties of the metal–organic frameworks Cu3(BTC)2 and UiO-66

5a. CONTRACT NUMBER
W911NF-10-1-0076

5b. GRANT NUMBER

5c. PROGRAM ELEMENT NUMBER
622622

6. AUTHORS

Gregory W. Peterson, Jared B. DeCoste, T. Grant Glover, Yougui Huang, Himanshu Jasuja, Krista S. Walton

5d. PROJECT NUMBER

5e. TASK NUMBER

5f. WORK UNIT NUMBER

7. PERFORMING ORGANIZATION NAMES AND ADDRESSES

Georgia Tech Research Corporation
Office of Sponsored Programs
505 Tenth Street NW
Atlanta, GA 30332 -0420

8. PERFORMING ORGANIZATION REPORT NUMBER

9. SPONSORING/MONITORING AGENCY NAME(S) AND ADDRESS(ES)

U.S. Army Research Office
P.O. Box 12211
Research Triangle Park, NC 27709-2211

10. SPONSOR/MONITOR'S ACRONYM(S)
ARO

11. SPONSOR/MONITOR'S REPORT NUMBER(S)
57994-CH.25

12. DISTRIBUTION AVAILIBILITY STATEMENT

Approved for public release; distribution is unlimited.

13. SUPPLEMENTARY NOTES

The views, opinions and/or findings contained in this report are those of the author(s) and should not contrued as an official Department of the Army position, policy or decision, unless so designated by other documentation.

14. ABSTRACT

The metal–organic frameworks CuBTC and UiO-66 were pressed at 1000 and 10,000 psi as a first step to engineering particles for use in toxic chemical removal applications. Materials characterization was conducted on each material using powder X-ray diffraction, attenuated total reflectance – Fourier transform infrared spectroscopy, and nitrogen porosimetry. Neither material showed signs of structural degradation during pressing. The CuBTC pressed materials show reduced porosity after pressing, while the UiO-66 surface area remained

15. SUBJECT TERMS

MOF; Cu3(BTC)2; HKUST-1; UiO-66; Particle

16. SECURITY CLASSIFICATION OF:			17. LIMITATION OF ABSTRACT	15. NUMBER OF PAGES	19a. NAME OF RESPONSIBLE PERSON
a. REPORT	b. ABSTRACT	c. THIS PAGE			Krista Walton
UU	UU	UU	UU		19b. TELEPHONE NUMBER: 404-894-5254

Report Title

Effects of pelletization pressure on the physical and chemical properties of the metal–organic frameworks Cu3(BTC)2 and UiO-66

ABSTRACT

The metal–organic frameworks CuBTC and UiO-66 were pressed at 1000 and 10,000 psi as a first step to engineering particles for use in toxic chemical removal applications. Materials characterization was conducted on each material using powder X-ray diffraction, attenuated total reflectance – Fourier transform infrared spectroscopy, and nitrogen porosimetry. Neither material showed signs of structural degradation during pressing. The CuBTC pressed materials show reduced porosity after pressing, while the UiO-66 surface area remained consistent for all pressed samples. Small-scale breakthrough testing was conducted with CuBTC against ammonia, which probes the reactive sites, and UiO-66 against octane, which probes physical adsorption capacity. Even with the decrease in surface area, the CuBTC materials had consistent ammonia removal capacities, while the UiO-66 pressed materials showed a slight decrease in octane loadings. Data indicate that pressing these MOFs into pellets without a binder is a viable approach to engineering particles in support of filtration and other applications.

REPORT DOCUMENTATION PAGE (SF298)
(Continuation Sheet)

Continuation for Block 13

ARO Report Number 57994.25-CH
Effects of pelletization pressure on the physical ...

Block 13: Supplementary Note

Approved for public release; distribution is unlimited.

Microporous and Mesoporous Materials 179 (2013) 48–53

Contents lists available at SciVerse ScienceDirect

Microporous and Mesoporous Materials

journal homepage: www.elsevier.com/locate/micromeso

Effects of pelletization pressure on the physical and chemical properties of the metal–organic frameworks $Cu_3(BTC)_2$ and UiO-66

Gregory W. Peterson [a,*], Jared B. DeCoste [b], T. Grant Glover [b], Yougui Huang [c], Himanshu Jasuja [c], Krista S. Walton [c]

[a] Edgewood Chemical Biological Center, 5183 Blackhawk Rd., Aberdeen Proving Ground, MD 21010, USA
[b] SAIC, Gunpowder, MD 21010, USA
[c] Georgia Institute of Technology, School of Chemical & Biomolecular Engineering, Atlanta, GA 30332, USA

ARTICLE INFO

Article history:
Received 11 January 2013
Received in revised form 16 February 2013
Accepted 18 February 2013
Available online 26 February 2013

Keywords:
MOF
$Cu_3(BTC)_2$
HKUST-1
UiO-66
Particle

ABSTRACT

The metal–organic frameworks CuBTC and UiO-66 were pressed at 1000 and 10,000 psi as a first step to engineering particles for use in toxic chemical removal applications. Materials characterization was conducted on each material using powder X-ray diffraction, attenuated total reflectance – Fourier transform infrared spectroscopy, and nitrogen porosimetry. Neither material showed signs of structural degradation during pressing. The CuBTC pressed materials show reduced porosity after pressing, while the UiO-66 surface area remained consistent for all pressed samples. Small-scale breakthrough testing was conducted with CuBTC against ammonia, which probes the reactive sites, and UiO-66 against octane, which probes physical adsorption capacity. Even with the decrease in surface area, the CuBTC materials had consistent ammonia removal capacities, while the UiO-66 pressed materials showed a slight decrease in octane loadings. Data indicate that pressing these MOFs into pellets without a binder is a viable approach to engineering particles in support of filtration and other applications.

1. Introduction

Sorbent design is an active field of study in a variety of commodity areas, including catalysis [1,2], gas storage [3,4], and separations [5,6]. Each of these areas requires specific micro- and macro-level properties. For example, chemical storage or removal may depend on a combination of physical properties, such as porosity and surface area, as well as chemical properties, such as reaction with surface groups. In all cases, materials must also be used in forms suitable for their host application, and engineered such that performance and energy (pressure drop) are optimized.

One of the more challenging applications for sorbent design is air purification and filtration. Due to the wide variety of chemicals that can be encountered, including highly toxic nerve agents, acidic/acid-forming gases such as chlorine, phosgene, sulfur dioxide, and hydrogen chloride, as well as basic gases such as ammonia, materials must be developed with several different functionalities capable of removing different classes of chemicals.

Metal–organic frameworks (MOFs) have been widely investigated over the past decade for use in these different applications [7–11]. MOFs combine metal nodes with organic linkers, forming extended nanoporous networks. They are of particular interest due to the wide variety of functionalities that can be combined to tune physical and chemical properties of the sorbent. One such material, UiO-66, is a promising MOF for several reasons. It is one of the most stable MOFs known, as it does not degrade in acids, many typical solvents, or due to moisture [12]. It can also be functionalized in a variety of ways, either during initial synthesis by using linkers with pendant groups [13–16], or post-synthesis using chemical reactions or exchange [17,18]. Because of these properties, UiO-66 is essentially a molecular scaffold that can be tuned depending on the application.

Another promising material, CuBTC (aka $Cu_3(BTC)_2$, or HKUST-1), has been extensively studied in a variety of applications [19,20]. Although this material is not stable to moisture [21], methods have been developed to stabilize the material, such as with a plasma-enhanced chemical vapor deposition of perfluorohexane [22]. Peterson and coworkers demonstrated the high efficiency of CuBTC for ammonia removal [23], and therefore this MOF is a prime candidate for incorporation into filtration applications.

Several previous efforts have examined pelletizing MOFs [24–27], including UiO-66 and CuBTC [12,28]; however, many involve pelletization with a binder [29,30], which inherently changes the properties of the material. Many of the efforts also fail to examine the changes to porosity, density, and other important engineering parameters [12], or investigate liquid sorption [28] as opposed to toxic chemical removal. In addition to binders, it is common to

* Corresponding author. Tel.: +1 (410) 436 9794.
E-mail address: gregory.w.peterson.civ@mail.mil (G.W. Peterson).

1387-1811/$ - see front matter © 2013 Published by Elsevier Inc.
http://dx.doi.org/10.1016/j.micromeso.2013.02.025

form pellets through the application of direct pressure on powders. The effect of pressure for forming MOF pellets on toxic chemical filtration capacity has not been extensively detailed in the literature. One recent effort by Kim and coworkers did in fact investigate using pressure with and without binders to create pellets of CuBTC [31]; however, X-ray diffraction data indicated the degradation of the structure at higher pressures. Moggach and coworkers investigated changes to the CuBTC crystal structure upon pressurization [32], while Cheetham and Tan reviewed the effect of pressure on variety of MOFs, including CuBTC [33].

This paper examines the first steps in materials engineering, with the objective of determining the effects of pressure during pelletization on the physical properties and chemical removal capabilities. UiO-66 and CuBTC were pressed at 1000 and 10,000 psi, followed by structural characterization and breakthrough testing.

2. Experimental

2.1. Materials synthesis

CuBTC was purchased from Sigma Aldrich, while UiO-66 was synthesized in-house. For the latter, 19.068 mmoles of zirconium (IV) chloride and 19.068 mmoles of benzene dicarboxyalate were mixed in 742 ml of dimethyl formamide (DMF) at room temperature in a glass beaker. The resulting mixture was divided in equal parts into three 500 ml glass jars. The jars were placed in a preheated oven at 120 °C for 24 h. The solution was cooled to room temperate, and the resulting solid was repeatedly washed with DMF. DMF was subsequently exchanged with methanol and then activated in a vacuum oven prior to forming particles.

2.2. Pellet and materials preparation

Pellets were prepared using a Carver Press. For UiO-66, two grams of powder were inserted into a 35 mm die and pressed at 1000 and 10,000 psi for one minute (UiO-66-P1000 and UiO-66-P10000, respectively). For CuBTC, two grams were loaded into the 35 mm die within a glove box, and then sealed in a plastic bag void of gases. The powder was pressed at 1000 and 10,000 psi for one minute within the plastic bag and removed within the glove box (CuBTC-P1000 and CuBTC-P10000 respectively). This procedure was conducted to keep moisture from destroying the crystal structure and porosity [21]. Each pellet was ground using a mortar and pestle within the plastic bag to make powders for breakthrough testing. In the case of CuBTC-P1000, the sample did not form a full pellet, and powder was still present in the die, indicating the pressure is not sufficient to provide an engineered material; nonetheless, the material was still evaluated for physical and chemical removal properties. In the materials pressed at higher pressures, materials were crushed to compare to virgin powder; however, it is possible to make engineered particles via crushing and sieving operations.

2.3. PXRD

Powder X-ray diffraction (PXRD) measurements were taken using a PANalytical X'Pert X-ray powder diffractometer with an X'celerator detector. Samples were scanned at 45 kV and 40 mA, using CuKα radiation ($\lambda = 1.54$ Å), a step size of $2\theta = 0.033°$ (10.08 s/step) over the 2θ range of 10–80°. Zero-background discs were used to minimize background scattering. PXRD patterns were processed using the Reflex module in Material Studio 5.5 by Accelrys.

2.4. Attenuated total reflectance – fourier transform infrared spectroscopy

Infrared transmission spectra were collected for samples using a Bruker Tensor 27 FTIR equipped with a Bruker Platinum attenuated total reflectance accessory with a single reflection diamond crystal. Scans were taken from approximately 4000 to 600 cm^{-1}. Sixteen scans were averaged, and resulting spectra were background subtracted and baseline corrected.

2.5. Nitrogen isotherm

Nitrogen porosimetry data were collected using a Quantachrome Autosorb 1C Analyzer. The UiO-66 samples were outgassed at 350 °C for approximately 24 h, and the CuBTC samples were outgassed at 150 °C for approximately 24 h. The surface area was calculated using the BET method [34], and the pore size distribution was calculated with non-local density functional theory (NLDFT) using a slit-pore carbon kernel. Total pore volume was calculated at a P/P_0 of 0.99, and the micropore volume was calculated using the Dubinin–Radushkevitch (DR) method.

2.6. Breakthrough testing

Breakthrough testing was conducted to assess the effect of pressure during pelletization on chemical removal performance. UiO-66 samples were evaluated against octane, while CuBTC samples were evaluated against ammonia. All samples were first activated at approximately 150 °C (CuBTC) to 170 °C (UiO-66) under dry flowing air for 1 h, and then loaded into 4 mm i.d. fritted glass tubes to a depth of 4 mm. Table 1 summarizes the test conditions. The ammonia microbreakthrough apparatus has been described previously [11,23]. Briefly, a ballast was pressurized with a known amount of ammonia, then mixed with a diluent stream at 0% relative humidity (RH) and atmospheric pressure at rates necessary to achieve a challenge concentration of 1,000 mg/m^3. The stream then passed through the fritted glass tube packed with sorbent. The effluent concentration was continuously monitored using a Hewlett Packard (HP) 5890 gas chromatograph equipped with a photoionization detector (PID). Octane testing was conducted in a similar fashion, with the exception of the feed delivery and effluent monitoring. Dry air was passed over octane in a saturator cell, creating a saturated vapor stream, and then mixed with a diluent stream to achieve a challenge concentration of 4,000 mg/m^3. Effluent monitoring was conducted with an HP GC equipped with a flame ionization detector (FID). The microbreakthrough system has an approximately standard deviation of 10%. Results are plotted on a weighted basis (min/g) to account for differences in density. Chemical loadings were calculated by integration of the area under the breakthrough curves.

Table 1
Microbreakthrough testing conditions.

Parameter	Ammonia system	Octane system
Temperature	20 °C	20 °C
RH	0% (−40 °C dew point)	0% (−40 °C dew point)
Adsorbent mass	~10–25 mg	~10–25 mg
Adsorbent volume	55 mm^3	55 mm^3
Flow rate	20 mL/min	20 mL/min
Challenge concentration	1000 mg/m^3	4000 mg/m^3

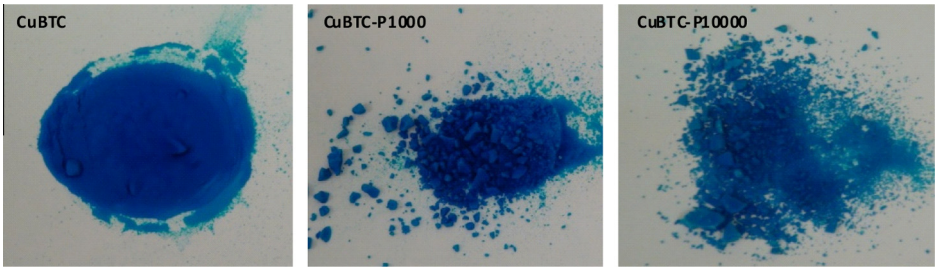

Fig. 1. CuBTC samples as-received, pelletized at 1000 psi, and pelletized at 10,000 psi. After pelletization, samples were crushed into small sizes to characterize.

Table 2
Surface area and pore volume measurements for CuBTC samples.

Sample	BET surface area (m^2/g)	Total pore volume (cc/g)	%Micropore volume (%)	Density (cc/g)
CuBTC	1698	0.75	93.7	0.30
CuBTC-P1000	1045	0.61	73.2	0.28
CuBTC-P10000	892	0.52	73.3	0.41

3. Results and discussion

3.1. CuBTC pelletization

The use of the die resulted in a disk, or pieces of a disk, approximately 35 mm in diameter. In order to characterize the materials the disk was broken into smaller pieces using a mortar and pestle. The powders were not crushed to a particular mesh size and were not sieved. Fig. 1 illustrates the crushed particles of CuBTC. As the pelletization pressure increases, the powder transforms into more discrete particles, taking on a more macro-crystalline form. The density of the materials was calculated by placing a known mass of material within a small graduated cylinder, and, as shown in Table 2, the density remains consistent for the as-received materials and the powders pressed at 1000 psi, but increases dramatically for materials pressed at 10,000 psi.

3.1.1. Physical properties characterization

Fig. 2 shows the powder X-ray diffraction data collected to ensure that the crystal structure remained intact after pelletization. Overall, the patterns are consistent for the three preparations, indicating that the crystal structures remain intact. However, the sig-

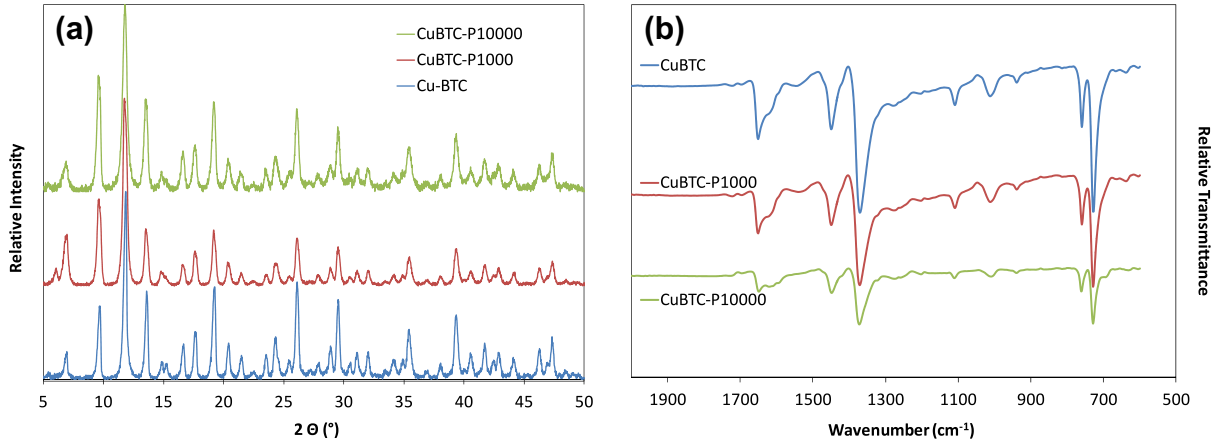

Fig. 2. (a) PXRD and (b) FTIR spectra for CuBTC samples.

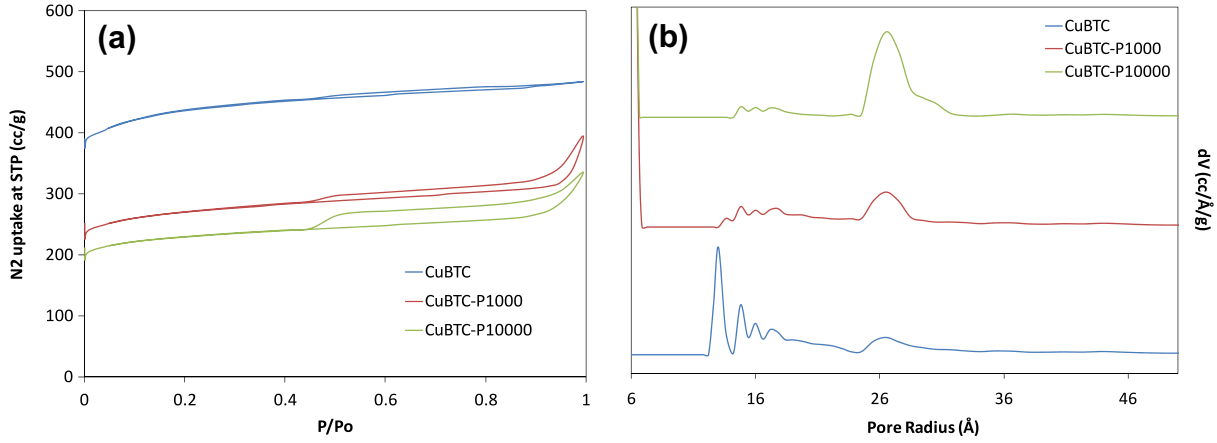

Fig. 3. (a) Nitrogen isotherms and (b) pore size distributions for CuBTC samples. As pelletization pressure increases, mesopores are formed within the material.

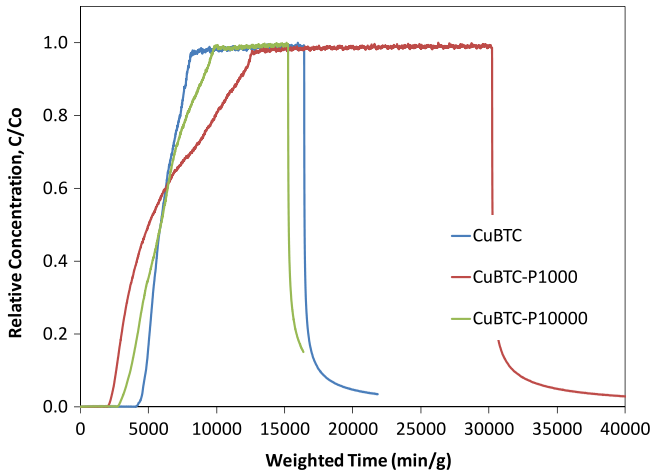

Fig. 4. Ammonia breakthrough results for CuBTC samples. Results show consistent ammonia removal for all three samples.

Table 3
Ammonia breakthrough results.

Sample	Loading (mmol/g)
CuBTC	7.2
CuBTC-P1000	7.2
CuBTC-P10000	7.1

nal-to-noise ratio decreases as the pressure increases, indicating at least partial structural collapse. To further ensure that the only changes to the powders were physical, and not chemical, FTIR spectra were collected, and are also shown in Fig. 2. The CuBTC exhibits the same spectra for all three preparations, indicating they remain structurally intact.

Nitrogen isotherms were collected to determine if porosity and pore size distribution were affected by the pelletization process. Fig. 3 illustrates the nitrogen uptake for the CuBTC samples, and Table 2 summarizes the BET surface area and pore volume of the three CuBTC samples. The as-received CuBTC exhibits a surface area consistent with the literature [35]. The as-received sample has the highest uptake, followed by the sample pressed at 1000 psi and finally the sample pressed at 10,000 psi. The decrease in surface area may be explained by localized pore structure collapse, which is supported by the reduced signal-to-noise of the CuBTC-P1000 sample. This is further supported by the development of mesopores, as seen by the hysteresis curves for the CuBTC-P1000 and especially the CuBTC-P10000 samples. Note the decrease in micropores and the increase in mesopores in the distribution plot of Fig. 3. It is possible that during the pelletization process, some bonds are broken, creating the mesopores.

Table 4
Surface area and pore volumes for UiO-66 samples.

Sample	BET surface area (m^2/g)	Total pore volume (cc/g)	%Micropore volume (%)	Density (cc/g)
UiO-66	1080	0.65	67.7	0.28
UiO-66-P1000	1080	0.66	63.3	0.28
UiO-66-P10000	1090	0.59	69.5	0.37

3.1.2. Ammonia microbreakthrough testing

CuBTC has previously been shown to provide excellent ammonia removal capabilities [23], and therefore samples were evaluated for their ammonia removal capabilities using a powder breakthrough system to determine the effects of pressing on performance. Fig. 4 illustrates the ammonia breakthrough curves. Results are plotted on a weighted basis to account for changes in density of the material. For both the pressed samples, ammonia begins eluting faster than the CuBTC as-received sample, possibly indicating issues of ammonia diffusing into the pores. The decreased sharpness of the breakthrough curves further supports diffusion resistance in the pressed samples. The total loading, as shown in Table 3, however, shows a consistent loading to saturation for all three samples. This indicates that, although the surface area and pore volume decrease with increasing pressure, the sites responsible for ammonia sorption are still accessible and active. Also of note is the sharp desorption curves, indicating ammonia is irreversibly adsorbed/reacted on the surface. The data shows that although the porosity decreases, pressing CuBTC into pellets does not degrade the total capacity of the material.

3.2. UiO-66 pelletization

Fig. 5 shows the crushed UiO-66 pellets, and Table 4 summarizes the surface area, pore volume, and densities of the materials. Note that, especially for the UiO-66-P10000 sample, the material is quite hard and retains significant macrostructure after crushing. Only the smallest granules were forwarded for octane testing. The density of the material also increases for the UiO-66-P10000 sample as compared to the UiO-66 material; however, the UiO-66-P1000 has a similar density to UiO-66.

3.2.1. Physical property characterization

Fig. 6 illustrates the PXRD data collected to determine changes to the crystal structure. It is apparent from the data that pressing the UiO-66 results in no change to the crystal structure. FTIR spectra indicate consistent functional groups between the samples, further indicating no chemical changes occurred during pressing.

Nitrogen isotherm data were collected to determine if the pelletization process affected the pore structure as is the case with CuBTC. Fig. 7 summarizes the nitrogen uptake and pore size distributions for the UiO-66 samples. Isotherm data for the samples indicate that pressure has little effect on the overall nitrogen up-

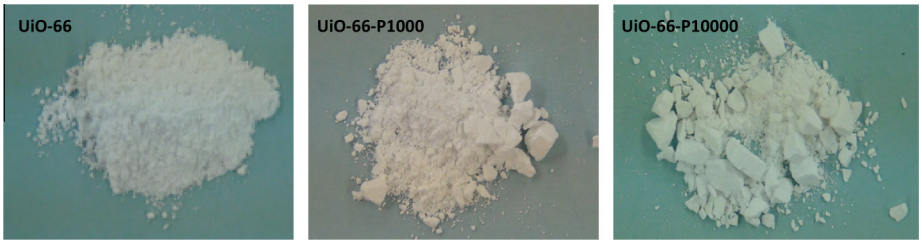

Fig. 5. UiO-66 samples as-received, pelletized at 1000 psi, and pelletized at 10,000 psi. After pelletization, samples were crushed into small sizes to characterize.

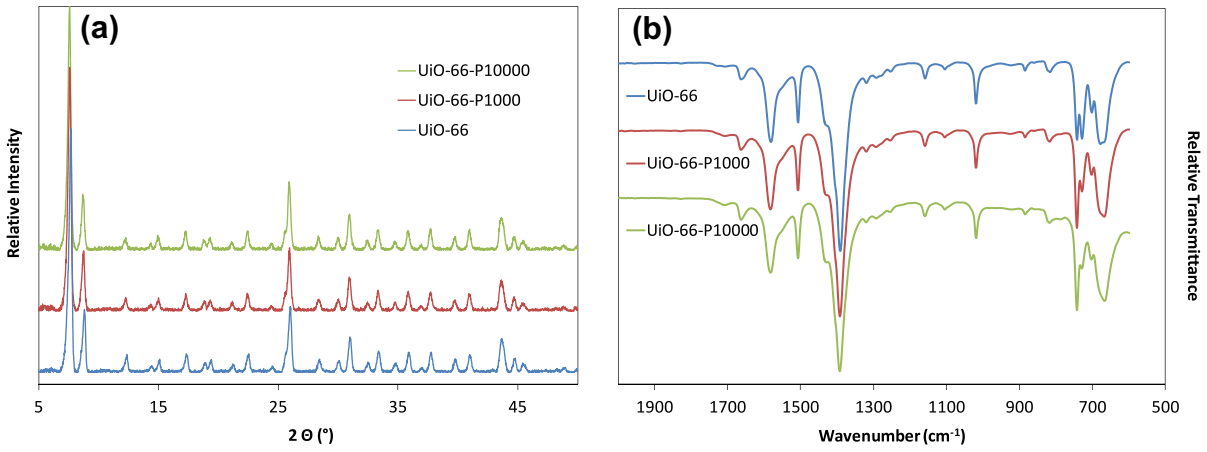

Fig. 6. (a) PXRD and (b) FTIR spectra for UiO-66 samples. Spectra for both techniques indicate no changes to the crystal structure or functional groups.

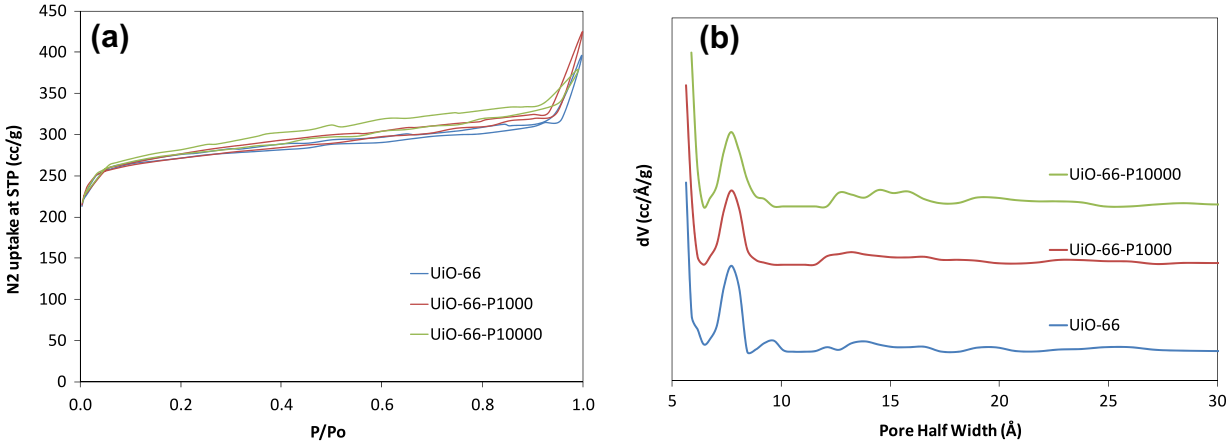

Fig. 7. (a) Nitrogen isotherm data and (b) pore size distributions for UiO-66 samples. Data indicate little effect of pressure on nitrogen uptake, but some increase in mesoporosity due to pressing.

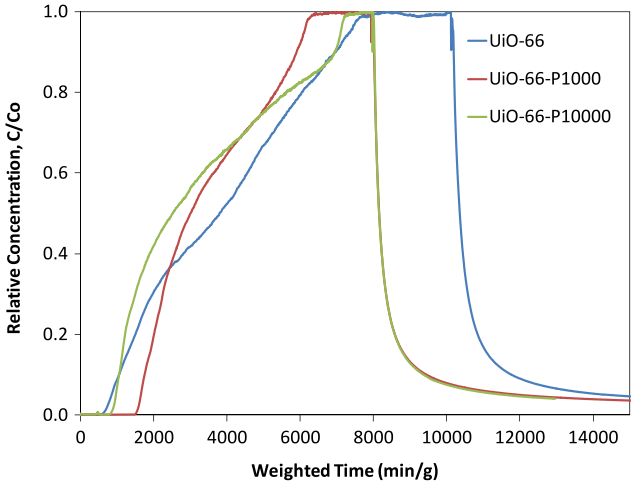

Fig. 8. Octane breakthrough results. The three samples tested show similar breakthrough behavior, indicating pelletization has limited effects on performance.

take, as all three isotherms are consistent throughout all relative pressures, within experimental error. The surface areas are also consistent for the three samples, although they are lower than previously reported values [36]. A reason for this is unknown, as the crystal structure is consistent with reported X-ray patterns; therefore, it may be due to activation procedure. The pore size distributions are also fairly consistent, although the powder UiO-66 sample shows slightly higher microporosity, with mesoporosity developing in the pressed samples. This behavior can be expected, as larger pores may be developed in between the crystals of the pressed structures during pelletization.

Table 5
Octane breakthrough results.

Sample	Loading (mmol/g)
UiO-66	2.5
UiO-66-P1000	2.3
UiO-66-P10000	2.1

3.2.2. Octane microbreakthrough testing

UiO-66 has limited functionality, and therefore octane was chosen as a test gas to evaluate the effects of pressure on performance. Powders were tested at a constant volume, with the mass varying according to changes in density from the pelletization process. Fig. 8 illustrates the results, which are plotted on a weighted time and relative concentration basis. Three replicates were tested for each sample. Surprisingly, the baseline UiO-66 sample exhibits octane breakthrough prior to the two pressed samples. However, all

three samples reach saturation at approximately the same weighted time. And, as shown in Table 5, the UiO-66 sample actually has the highest octane adsorption capacity, with capacity decreasing as pelletization pressure increases. Even after pressing at 10,000 psi, however, the material still retains significant octane removal capacity. These results are consistent with the nitrogen isotherm data, which show little or no change in porosity and surface area of the materials after pelletization.

4. Conclusions

The metal–organic frameworks CuBTC and UiO-66 were pressed at 1000 and 10,000 psi as a first step to engineering particles for use in chemical removal applications. In both cases, PXRD and FTIR data indicate that the crystal structures remain intact after pressing. The surface area and porosity of CuBTC decrease significantly after pressing, whereas the pressure has much less of an effect on UiO-66. Although the CuBTC material exhibited reduced porosity, the ammonia removal performance was unaffected, indicating that engineering CuBTC into hard granules is possible without detrimental effects. Octane breakthrough results do indicate degradation in performance for the UiO-66 material, but even the sample pressed at 10,000 psi still retains significant removal capacity.

Results from the study indicate that indeed both CuBTC and UiO-66 can be engineered into forms suitable for chemical removal applications. Although some degradation in porosity is seen for the samples, both still exhibit substantial chemical removal capabilities after pelletization. Further studies will be conducted to optimize hardness and density for larger-scale testing.

Acknowledgements

This work was completed through funding by the Defense Threat Reduction Agency under Project BA07PRO104 (ECBC) and ARO Contract Number W911NF-10-0076 (KSW). The authors thank Matthew Browe and Paulette Jones for conducting the breakthrough testing.

References

[1] S. Sato, Y. Yoshihiro, Y. Hidenori, M. Noritaka, M. Iwamoto, Applied Catalysis 70 (1991) L1–L5.
[2] A. Corma, M.S. Grande, V. Gonzalez-Alfaro, A.V. Orchilles, J. Catal. 159 (1996) 375–382.
[3] J.L.C. Rowsell, O.M. Yaghi, J. Am. Chem. Soc. 128 (2006) 1304–1315.
[4] Q. Yang, C. Zhong, J. Phys. Chem. B 110 (2006) 655–658.
[5] J. Padin, R.T. Yang, Chem. Eng. Sci. 55 (2000) 2607–2616.
[6] X. Xiaochun, S. Chunshan, B.G. Miller, A.W. Scaroni, Ind. Eng. Chem. Res. 44 (2005) 8113–8119.
[7] T. Duren, L. Sarkisov, O.M. Yaghi, R.Q. Snurr, Langmuir 20 (2004) 2683–2689.
[8] A.R. Millward, O.M. Yaghi, J. Am. Chem. Soc. 127 (2005) 17998–17999.
[9] J.G. Vitillo, L. Regli, S. Chava, G. Ricchiardi, G. Spoto, P.D.C. Dietzel, S. Bordiga, A. Zecchina, J. Am. Chem. Soc. 130 (2008) 8386–8396.
[10] A.G. Wong-Foy, A.J. Matzger, O.M. Yaghi, J. Am. Chem. Soc. 128 (2006) 3493–3495.
[11] T.G. Glover, G.W. Peterson, B.J. Schindler, D. Britt, O. Yaghi, Chem. Eng. Sci. 66 (2011) 163–170.
[12] J.H. Cavka, S. Jakobsen, U. Olsby, N. Guillou, C. Lamberti, S. Boriga, K.P. Lillerud, J. Am. Chem. Soc. 130 (2008) 13850–13851.
[13] M. Kandiah, M.H. Nilsen, S. Usseglio, S. Jakobsen, U. Olsbye, M. Tilset, C. Larabi, E.A. Quadrelli, F. Bonino, K.P. Lillerud, Chem. Mater. 22 (2010) 6632–6640.
[14] Y. Huang, W. Qin, Z. Li, Y. Li, Dalton Trans. 41 (2012) 9283–9285.
[15] G.E. Cmarik, M. Kim, S.M. Cohen, K.S. Walton, Langmuir 28 (2012) 15606–15613.
[16] H. Jasuja, J. Zang, D. Sholl, K.S. Walton, J. Phys. Chem. C 116 (2012) 23526–23532.
[17] S.J. Garibay, S.M. Cohen, Chem. Comm. 46 (2010) 770–7702.
[18] M. Kandiah, S. Usseglio, S. Svelle, U. Olsbye, K.P. Lillerud, M. Tilset, J. Mater. Chem. 20 (2010) 9848–9851.
[19] S.S.Y. Chui, S.M.F. Lo, J.P.H. Charmant, A.G. Orpen, Science 283 (1999) 1148–1150.
[20] B. Xiao, P.S. Wheatley, X. Zhao, A.J. Fletcher, S. Fox, A.G. Rossi, I.L. Megson, S. Bordiga, L. Regli, K.M. Thomas, R.E. Morris, J. Am. Chem. Soc. 129 (2007) 1203–1209.
[21] P.M. Schoenecker, C.G. Carson, H. Jasuja, C.J.J. Flemming, K.S. Walton, Ind. Eng. Chem. Res. 51 (2012) 6513–6519.
[22] J.B. DeCoste, G.W. Peterson, M.W. Smith, C.A. Stone, C.R. Willis, J. Am. Chem. Soc. 134 (2012) 1486–1489.
[23] G.W. Peterson, G.W. Wagner, A. Balboa, J. Mahle, T. Sewell, C.J. Karwacki, J. Phys. Chem. C 113 (2009) 13906–13917.
[24] M. Tagliabue, C. Rizzo, R. Millini, P.D.C. Dietzel, R. Blom, S. Zanardi, J. Porous Mater. 18 (2011) 289–296.
[25] J. Liu, J. Tian, P.K. Thallapally, B.P. McGrail, J. Phys. Chem. C 116 (2012) 9575–9581.
[26] J. Liu, Y. Wang, A.I. Benin, P. Jakubczak, R.R. Willis, M.D. LeVan, Langmuir 26 (2010) 14301–14307.
[27] J. Liu, P.K. Thallapally, D. Strachan, Langmuir 28 (2012) 11584–11589.
[28] P.S. Barcia, D. Guimaraes, P.A.P. Mendes, J.A.C. Silva, V. Guillerm, H. Chevreau, C. Serre, A.E. Rodrigues, Microporous Mesoporous Mater. 139 (2011) 67–73.
[29] V. Finsy, L. Ma, L. Alaerts, D.E. De Vos, G.V. Baron, J.F.M. Denayer, Microporous Mesoporous Mater. 120 (2009) 221–227.
[30] L.D. O'Neill, H. Zhang, D. Bradshaw, J. Mater. Chem. 20 (2010) 5720–5726.
[31] J. Kim, S.-H. Kim, S.-T. Yang, Microporous Mesoporous Mater. 161 (2012) 48–55.
[32] A.J. Graham, J.-C. Tan, D.R. llan, S.A. Moggach, Chem. Commun. 48 (2012) 1535–1537.
[33] J.C. Tan, A.K. Cheetham, Chem. Soc. Rev. 40 (2011) 1059–1080.
[34] K.S. Walton, R.Q. Snurr, J. Am. Chem. Soc. 129 (2007) 8552–8556.
[35] M. Hartmann, S. Kunz, D. Himsl, O. Tangermann, S. Ernst, A. Wagener, Langmuir 24 (2008) 8634–8642.
[36] H.R. Abid, H. Tian, H.-M. Ang, M.O. Tade, C.E. Buckley, S. Wang, Chem. Eng. J. 187 (2012) 415–420.